Received: 17 April 2017 | Revised: 28 September 2017 | Accepted: 9 October 2017

DOI: 10.1002/stc.2120

RESEARCH ARTICLE

WILEY

Development of a smart-device-based vibration-measurement system: Effectiveness examination and application cases to existing structure

Ashish Shrestha[1] | Ji Dang[1] | Xin Wang[2]

[1] Department of Civil and Environmental Engineering, Saitama University, Saitama City, Japan

[2] International Research Institute of Disaster Science, Tohoku University, Sendai City, Japan

Correspondence
Ashish Shrestha, Department of Civil and Environmental Engineering, Saitama University, Saitama City, Japan.
Email: ashishduwaju@hotmail.com

Summary

After the 2011 Great East Japan Earthquake, long-term vibration measurement using high-density instruments is one of the most critical issues for structural-health-monitoring owing to increasing deterioration and threat of future large earthquakes. Because of the high initial and running costs of traditional monitoring systems, smart-device-based measurement system is considered as a simple and easy solution. In this paper, the effectiveness of in-built sensor, data transfer via wireless local area network, data acquisition to a synchronize cloud server, and trigger function using shaking table tests were firstly examined. A measurement system including a group of sensors has been established successfully based on the "control center" from which the trigger command can be send to other sensors immediately as any sensor/sensors is/are triggered. Then, the system is applied to seismic-response and environment-vibration measurement at existing structures. Results show that the observable acceleration level of smart devices is more than 5 gal in the frequency range of 0.1 to 10 Hz. The possible sampling rate is 100 Hz. Though it is unstable, correction methods have been proposed. Continuous measurement and data transfer is possible without data loss. Dynamic properties extracted from smart-device-based system is very similar to those extracted from high-quality-sensor-based system.

KEYWORDS

dense structural measurements, MEMS accelerometers, performance verification, shaking table tests, smart devices, structural health monitoring

1 | INTRODUCTION

In recent decades, major earthquakes in Japan have damaged numerous buildings, bridges, and other civil infrastructure. Collapse of highway bridges during the 1995 Hanshin-Awaji Earthquake paralyzed the function of transportation in urban areas, greatly hindering the post-earthquake recovery process.[1–3] Although knowing the real seismic responses with nonlinear hysteresis behavior in both structures and soil is important for reducing disaster severity and improving urban infrastructure systems' resilience, damage-related instrumental records are very rare, as only very few structures include seismic-monitoring systems. Thus, attempts to simulate the seismic damage to bridges through large-scale shaking-table tests have been conducted.[4,5] However, only very few representative cases are available for such tests, and interpreting the data is extremely difficult.[6] Damage related to seismic waves or structural-character

uncertainty, such as bidirectional-wave interactions or rubber-bearing deterioration, are difficult to experimentally clarify.

After the 2011 Great East Japan Earthquake, much research has been conducted to identify the reasons for damages to structures, such as Shinkansen derailment[7] and breaking of rubber bearings[8] based on ground-motion records of nearby strong-motion-sensing networks. However, the final verification of these analysis and experiments should be based on real instrumental records of structural response, as the previous research was based on many simplifying assumptions and generally agreed with only some parts of the damage observations. Without such records, neither structural damage nor the behavior of structures during strong earthquakes can be used to improve the seismic-design criteria. At present, it is only possible to determine certain static factors contributing structural failure, such as insufficient strength or ductility, uncertainty of the material's initial strength and deterioration status; other probable dynamics-related factors such as site amplification of input ground motion, structural soil interaction, and bidirectional interactions are either too difficult or too expensive to identify as reasons for structural seismic damage by current analytical or experimental methods. One of the most straightforward ways to obtain such useful information is to establish a dense structural-response network by installing a greater number of instruments in infrastructures in seismicity-prone areas such as Japan.

Although seismometers have been utilized in structural-health monitoring (SHM) systems[9], the initial and running costs for such systems are too high for transportation infrastructure such as highway or railway viaducts. Until now, the application of such systems is limited only to some of the most important infrastructure. From a long-term perspective aiming to observe the seismic responses of a large group of structures and to ensure a great deal of valuable seismic-response data, development and utilization of highly practical observation systems that can be maintained at low cost is a major challenge.

Microelectromechanical-system (MEMS)-based measurements have been applied to SHM systems for bridges, using such techniques as wireless sensors[10,11] or dense earthquake and SHM systems such as the Community Seismic Network[12]. However, in general, these systems have limited resources, due to which it is often difficult to properly apply them[13,14], and the compounded use of different components to build such systems is not easy and increases the overall cost as well.

With increase in central processing unit capabilities, improvements in built-in MEMS accelerometers, and easy offline or online programmable functionality, smart devices have come to be seen as possible options for acceleration sensors, data-restoring and cloud-sharing devices, and time-synchronized computers. Using smart devices as a platform can also shorten the development cycle and minimize its cost. A new system for measuring the structural seismic response, evaluating seismic safety, and quickly determining the seismic-damage level after large earthquakes can be easily developed using only some smart devices operating special applications. Servo-type or MEMS-type sensor-based systems are generally built for special users such as scholars or engineers and with one dimensional use, that is, for sensing only. The motivation to improve usability and user experience and performance of such sensors is not as high as other commercial electronic devices such as smartphones. Japan has the most dense network for earthquake observation (installed by K-NET, KiK-net), yet the numbers are limited to capture accurate response during earthquakes. Therefore, their use is limited, development cost is very high per device, and it is very difficult to use such system especially in case of developing or underdeveloped nations. Motivation to develop such system on a global basis thus seems minimum. On the other hand, smart devices are cheap, multidimensional, open, and programmable that is fit with the features of traditional smart sensors.[15] In addition to sensing, these devices come with computing and communication resources that offer a low barrier of entry for third-party programmers (e.g., undergraduates with little programming experience can develop and ship applications). More importantly, smart device vendor now offers an app store allowing developers to deliver new applications to large populations of users across the globe, which is transforming the deployment of new applications and allowing the collection and analysis of data far beyond the scale of what was previously possible. Over 1 billion smart devices are produced each year,[16] which means, they could constitute a very robust large data-sending network that could easily be used in both developed and developing countries with user-friendly user interfaces. With a simple guide, everyone can operate smartphone apps easily.

Although few studies have been conducted to test the performance of the MEMS sensors' built-in smart devices,[17–23] the performance of these devices in measuring structural vibration has not been verified before its practice in real structural monitoring or seismic-response recording. Moreover, for structural-vibration measurement, the following are the most important performance indicators of concern to structural engineers that have not yet been evaluated:

1. Error level and noise in acceleration measurement;
2. Accuracy and reliability of frequency and amplitude measurements;

3. Possible sampling rate;
4. Reliability of such devices over long-term use;
5. How to restore and transport data stably and safely

Therefore, this study attempts to illustrate the effectiveness of smart-device-based structural seismic monitoring in more detail by addressing the above-mentioned issues. For the purpose of structural-seismic-response recording, an acceleration-measurement smart-device application was developed. With this application, acceleration data sampled by the built-in MEMS-accelerometer sensor was recorded, and the data file was synchronized with the cloud server, such that those data could be accessed by remote terminals. Shaking-table tests were conducted to clarify the performance of smart devices such as smartphones, tablet computers, and media players using the developed application program. The performance of smart-device-based structural-vibration measurement, according to such metrics as noise level, reliable measurement ranges of amplitude and frequency, and possible sampling rate, were evaluated based on the test results of each device. The long-term sustainable-measurement performance of the developed application was also tested by a long-term building-structural measurement, and several seismic events were captured successfully. On-site environmental-vibration testing using smart devices and reference sensors was also conducted to verify the feasibility of the method for onsite implementation.

2 | SMART-DEVICE-BASED VIBRATION-MEASUREMENT METHOD

2.1 | Application development environment

The built-in MEMS sensor is the fundamental element that gathers acceleration data and requires feedback for its operation. An interconnecting infrastructure network as shown in Figure 1 is required to communicate and process the information required for services and monitoring applications, which are generally done by the operating system. The operating system is designed to make these sensor components available to apps through application-programming interfaces (APIs). Apps are software applications for smart devices, often designed for specific tasks, which can interact with hardware and operating-system features. Apps are responsible for acquiring data, analyzing data, storing data, and transferring useful data to the cloud. The app was developed based on the Objective-C programming language in the integrated development environment Xcode.

A sample application project "MotionGraphs"[24] was used as the primary application program for sensing the motion/vibration events. It demonstrates how to receive acceleration-measurement data from core motion and displays graphs of the accelerometer, gyroscope, and device-motion data.

2.2 | Data acquisition and storage

In this study, the Dropbox sync API[25] is used as the data-restoring cloud server. A data file is firstly recorded in the memory and stored to the local folder; once an internet connection, Wi-Fi, or cellular network is available, it will be

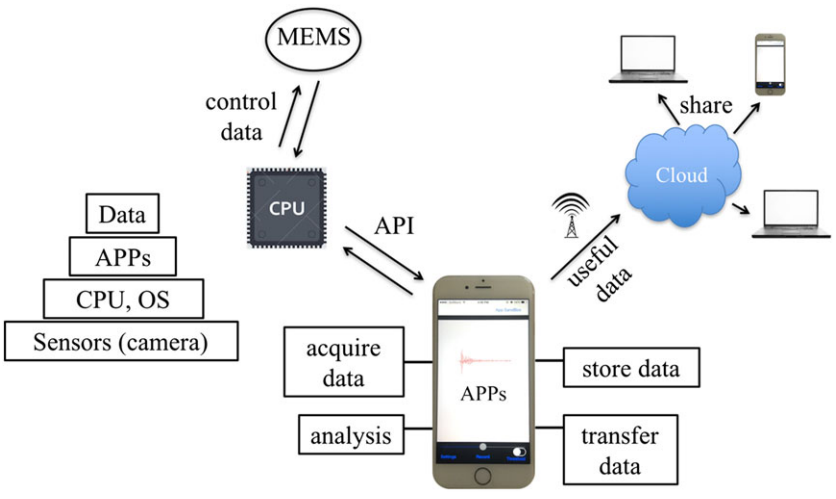

FIGURE 1 Measurement-application-program development using smart devices. API = application-programming interface; CPU = central processing unit; MEMS = microelectromechanical-system; OS = operating system

uploaded to the cloud server safely. Using the Dropbox sync API, the app can share its file system with the Dropbox client running in the background, such that the app can read, create, and modify files. It also notifies the app when the parameter-setting file in the cloud server is changed by other terminals, such that the app can respond instantly and synchronize its measurement settings to the newest command.

2.3 | User interface and data processing

The app is, primarily, a continuous vibration-sensing process with a single recording function for single measurement, multiple recording functions for long-term 24-hr monitoring, and a seismometer function for ground-motion observation with a trigger. Figure 2a shows the basic user interface of the developed acceleration-measurement-application program, whereas Figure 2b and 2c show the basic operational flow of the above-mentioned functions.

Measurement records can be initiated manually, as shown in Figure 2b, or by a trigger, as shown in Figure 2c. The single- and multiple-recording modes are both manual modes triggered by buttons. In both cases, the user controls when to start or stop the recording process. However, a single-recording mode is suitable for short-term recordings, and only one recording event at a time occurs between switching the start-stop buttons. The multiple-recording mode is suitable for long-term recordings, whereby a single recording event between switching the start-stop button is subdivided into multiple files such that the system does not have to allocate large amounts of memory to process a single large data file, thus ensuring that the program does not crash occasionally.

In this study, for practical structural observation, a ground-motion-observation function using the trigger recording mode was developed. In the seismometer mode, only some short-term buffering over time T_b stays in the memory; once the buffering data trigger a recording event, a new recording will be initiated with buffered data automatically, as shown in Figure 2c. The triggered recordings will end themselves when shaking desists (i.e., when a duration T_b passes without triggering events). Here, the amplitude trigger is used, and the threshold is set to 10 gal.

3 | PERFORMANCE EXAMINATION USING SHAKING-TABLE TESTS

To identify the reliable utility range of smart devices for structural-vibration measurement, two sets of shaking-table tests were carried out using two different shaking tables, as shown in Figure 3. The first set of tests was conducted by a uniaxial small-harmonic-excitation shaking table (APS-113, Figure 3a) with different frequencies and amplitudes. The second set of tests was carried out by applying ground motion of varying intensities to another shaking table (SSV-125, Figure 3b). Technical specification of these shaking table is shown in Table 1.

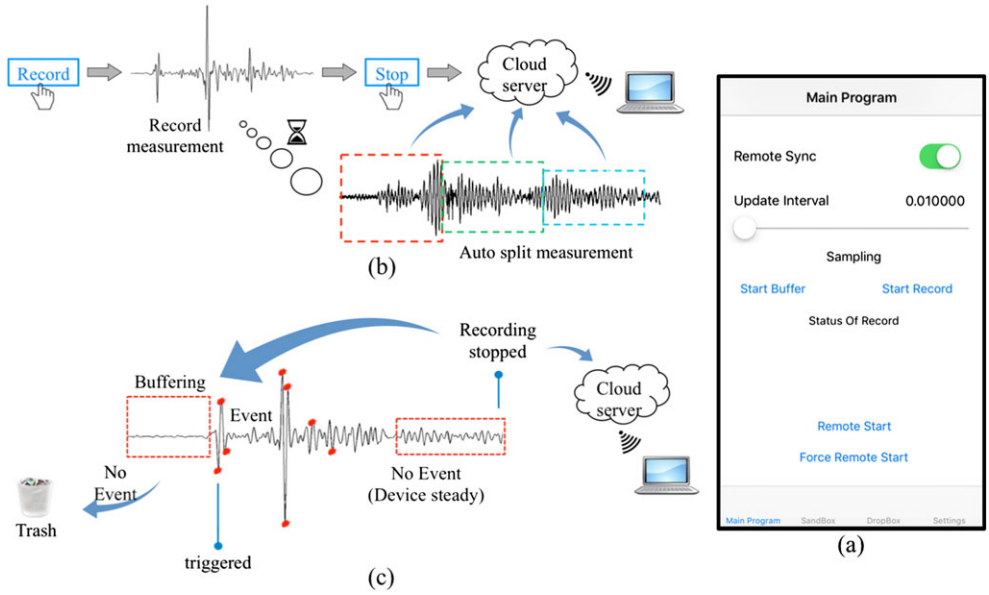

FIGURE 2 (a) Program user interface, (b) manual-recording functionality within the application, and (c) triggered recording functionality within the application

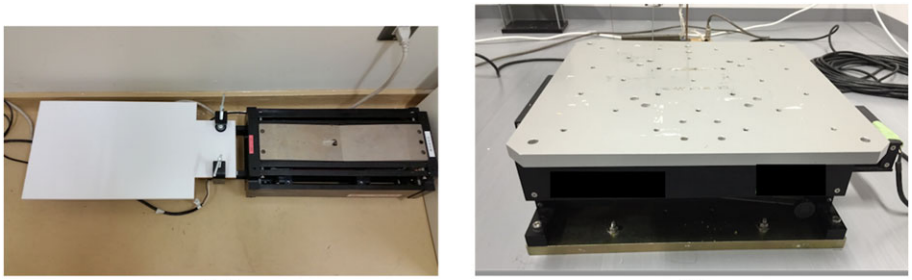

FIGURE 3 (a) Uniaxial shaking table (APS-113) and (b) uniaxial shaking table (SSV-125)

TABLE 1 Shaking-tables specification [26,27]

Property	APS-113	SSV-125
Maker	APS dynamics, INC.	SAN ES Corporation
Maximum excitation force (N)	133	490
Maximum displacement ($mm^{P\text{-}P}$)	158	150
Maximum speed (mm/s)	1000	1000
Frequency range (Hz)	0.1–200	0.1–1000
Mass (kg)	36	48
Dimension $L \times W \times H$ (mm)	526 × 213 × 168	520 × 280 × 170

3.1 | Specimens

The reference-measurement system, as shown in Figure 4a, consists of a high-quality servo-velocity sensor as a reference sensor and five other widely used smart devices embedded with different MEMS accelerometers as specimens. The basic characteristic of each MEMS accelerometer and the reference sensor is shown in Table 2.

The MEMS accelerometers inside of smart devices can sample stably at a maximum frequency of 100 Hz (corresponding to a Nyquist frequency of 50 Hz). This sampling frequency is generally considered sufficient for most engineering applications, including ground-shaking or structural-response measurement, and in addition, all of these smart devices are equipped with a Global Positioning System (GPS) unit to track the location of record as well.

3.2 | Loading and measurement equipment

Figure 4a shows the test specimen layout on the shaking table. The uniaxial shaking table (APS-113) was used to simulate sinusoidal oscillation. The SVA-ST-30 amplifier amplified the input excitation of the shaking table, and the WF-1974

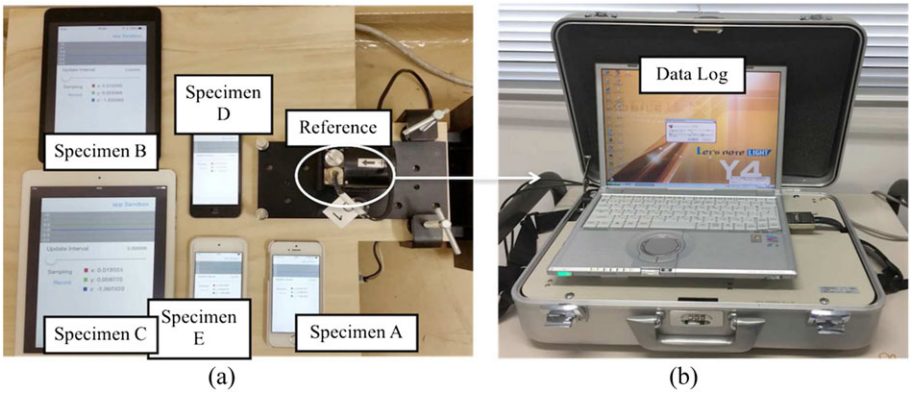

FIGURE 4 (a) Shaking table set up for the sinusoidal test and (b) data log for the reference-measurement system

TABLE 2 Reference sensor and smart-device sensor properties [28–32]

Specimen code		A	B	C	D	E
Property	Reference	iPhone 5 s	iPad Mini 2	iPad Air 2	iPod Touch—4	iPod Touch—2
Sensor maker	Tokyo Sokushin co. ltd.	Bosch Sensortech	STMicroelectronics	Bosch Sensortech	STMicroelectronics	
Sensor model	VSE-15D	BMA220	LIS331DLH	BMA280	LIS331DLH	
Sensor type	Servo velocity sensor	MEMS	MEMS	MEMS	MEMS	
Sensitivity	5000 mV/g	16 LSB/g	1000 LSB/g	4096 LSB/g	1000 LSB/g	
Resolution (gal)	10^{-5}	2	2.18	1.20	2.18	
Acceleration range (g)	±2	±2/±4/±8/±16	±2/±4/±8	±2/±4/±8/±16	±2/±4/±8	

Note. MEMS = microelectromechanical-system

function generator served sinusoidal waves to the table as input. A data log, as shown in Figure 4b, was used to collect data from a reference sensor.

To investigate the smart device's capability to measure structural seismic vibration of different frequencies and amplitudes, sinusoidal shaking-table tests with frequencies from 0.1 to 10.0 Hz and amplitudes from 5 to 150 gal were conducted, as shown in Table 3.

3.3 | Deviation of sampling frequency and error correction

In each test, five different smart devices were placed on the shaking table, along with high-quality reference-measurement device. Tape is used in this experiment as a quick and easy method of mounting smart devices. The stiffness of tape is therefore important to obtain robust data, which was confirmed through following methods:

1. Visual confirmation: After fixing the devices, the strength of adhesive force of tape was checked by applying forced-manual movement, and in case of insufficient adhesion, more tapes were applied to ensure stability and no relative movement between the devices and the table.
2. Response of devices: Time history response and frequency response of acceleration measurement shown in Figure 8 also verifies that the fidelity of measurement response has not been compromised by the use of double-sided tape. There is no time lag or difference in the dominant frequency component identified from smart devices with that of reference sensor.

The sampling rate of smart devices were set to 100 Hz. The sinusoidal motions recorded by five different devices were compared with that recorded by the reference sensor in terms of acceleration waveforms and the Fourier amplitude spectrum. The acceleration waveform measured by the smart device and reference sensor for a sine wave of 2-Hz frequency with an amplitude of 10 gal is shown in Figure 5a and 5b, respectively, as an example.

As shown in the figure, the waveforms measured by the high-precision reference sensor and the smart device are generally similar. However, the time lag in the waveform is also observed, and there is also a gap in the primary frequency of the motion in the Fourier-amplitude spectrum. Similar observations were found in results for other devices as well. To determine the reason of this gap, the recording time of each sample was checked, and it was found that the

TABLE 3 Sinusoidal shaking table tests setting

		Frequency(Hz)						
		0.1	0.2	0.5	1	2	5	10
Amplitudes (gal)	±5	S11	S12	S13	S14	S15	S16	S17
	±10	S21	S22	S23	S24	S25	S26	S27
	±50	S31	S32	S33	S34	S35	S36	S37
	±100	S41	S42	S43	S44	S45	S46	S47
	±150	S51	S52	S53	S54	S55	S56	S57

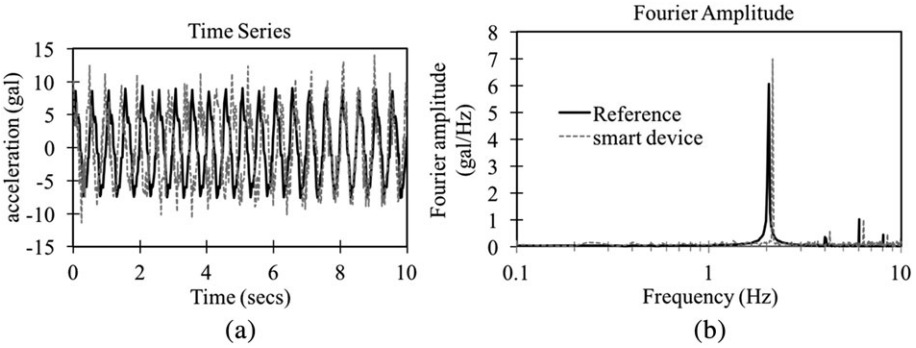

FIGURE 5 (a) Waveform and (b) Fourier-amplitude spectrum measured by Specimen D; the with frequency of the shaking table set to 2 Hz and the amplitude set to around 10 gal

time differences between samples were nearly 0.01 s but always with small errors. This error in sampling timing is random, and the randomness seems to differ in each device. This time lag of the measured waveform is the result of deviation in the sampling frequency.

Although a sampling rate of 100 Hz is set for all devices, the actual sampling rate offered by each device slightly deviated, as summarized in Figure 6b. A number of factors, including delays in the operating-system-level-time-stamp attachment to sensor measurements and instantaneous input/output loading, affect both the actual and reported sampling rates of sensors on the device. For example, heavy multitasking and input/output loading on smart devices, as exhibited in typical usage scenarios, may lead to unstable sampling rates and prevent the accelerometer data from being sampled at equal intervals. The sampling rates of Specimen D were counted for 100 s, and, by ordering the real sampling rate, the exceedance probability of the sampling rate could be observed as the Gaussian distribution shown in Figure 6a.

The expected values and deviations of sampling rates can be calculated from the probability ranges. Averages and deviations for all smart devices are plotted in Figure 6b. However, the average and deviation of a given device also somehow varies with in each measurement. It can be seen from the figure that Specimen C is the most stable smart device and has the most accurate sampling rate with the least variation. On the other hand, the average values of the sampling rates of Specimens D and E are much larger than the set target, the variation is large, and the sampling rate is largely unstable. Therefore, from the figure, it can be seen that newer smart devices can be expected to offer more reliable measurements due to the higher performance of their central processing units.

As the data-collecting time is random, the sampling rate is unstable. There are several numerical methods, such as data resampling or use of the real sampling time, to correct this error. The simplest way is just use the average sampling rate, $\overline{f_a}$:

$$\overline{f_a} = N_s/T_s \tag{1}$$

Here, N_s is the total number of samples in a record, and T_s is the total duration recorded according to the smart devices. Thus, the average time interval $\overline{\Delta t}$ can be used as the records' time interval, where $\overline{\Delta t}$ is the inverse of the record's average-sampling rate:

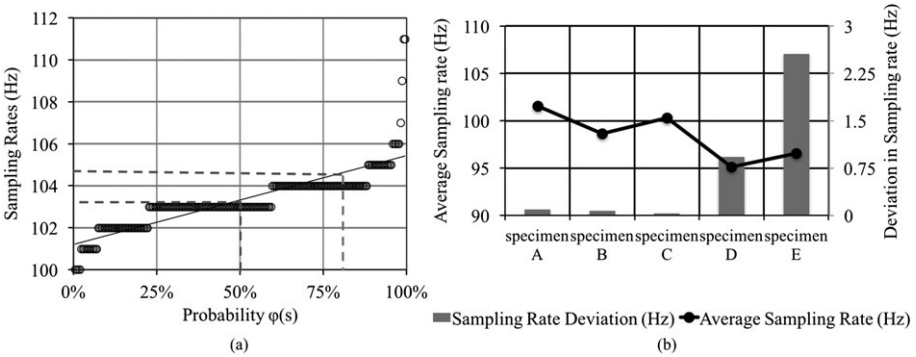

FIGURE 6 (a) Probabilities of sampling rates of Specimen D and (b) sampling-rate characteristics of different smart devices

$$\overline{\Delta t} = 1/\overline{f_a}. \tag{2}$$

The internal clock of the smart device will be synchronized with the network-time-protocol server when it is online. The time error is very small. To verify the viability of this method, the time history and Fourier-amplitude spectrum of the reference and corrected specimen records are compared, as shown in Figure 7. It can be seen that there is no substantial difference in the dominant frequencies seen in the Fourier-amplitude-spectrum plot.

Another convenient method for regulating the sampling rate is to resample the data by interpolating from the raw data. Unification to a common target rate, as a preprocessing step, ensures that all interpolated samples in each data window will be equidistantly separated in time. In order to verify the reliability and accuracy of the interpolated resampled data, comparison of resampled data (measured by smart devices) and reference data (measured by servo-velocity sensors) was performed as shown in Figure 8.

It can be seen that the resampled waveform agrees very well with the reference waveform (more accurately than in the previous method, that is, by taking the average sampling rate), and the Fourier-amplitude spectrum, in each periodic component, shows no great difference between the two. This suggests that the interpolation technique could be an effective method of correcting the sampling-rate-deviation problem. With interpolation, a regularly sampled signal is extracted from observations that are irregularly spaced in time.

3.4 | Sinusoidal-excitation tests

After data correction, the primary frequency and corresponding amplitude for each test can be identified from their Fourier-amplitude spectra, as seen in Figures 7 and 8. This is the key information for SHM in future applications.

Figure 9a and 9b summarizes all test results for the frequency ratio and the amplitude ratio between the reference sensor and the smart devices (smart devices/reference), respectively. It can be seen that the smart devices, with respect to the reference sensor, are capable of accurately measuring the dominant frequency with an error below 0.1%, as seen in Figure 9a. However, from Figure 9b, it can be seen that smart devices tend to overestimate the amplitude of vibration for low-frequency signals (generally, signals with frequencies below 0.5 Hz). Nevertheless, for high-frequency signals (above 0.5 Hz), smart devices are reasonably accurate in measuring the amplitude of vibration as well. Similar results were obtained for all tests, with sinusoidal amplitude varying from 5 to 150 gal. This may be influenced by the pink noise of the MEMS, which is proportional to $1/f$. It can be corrected by a frequency-domain window directly if the low-frequency-domain data becomes important, for example, for high-rise-building or long-span-bridge monitoring. However, this works is outside of the scope of this research. Study by Amick et al.[33] demonstrates consistent sensitivity values across various smart devices with low coefficient of variability. Inspection of the acceleration data across the devices indicated the mean accelerations from different experiments to be very consistent with extremely small standard deviations. Similar results can be observed in this set of experiment as well. The acceleration data across different devices shows consistent sensitivity with amplitude increase as depicted in Figure 9c. Therefore, as verified below, general-purpose vibration-response measurement of a structure can be satisfied without further correction.

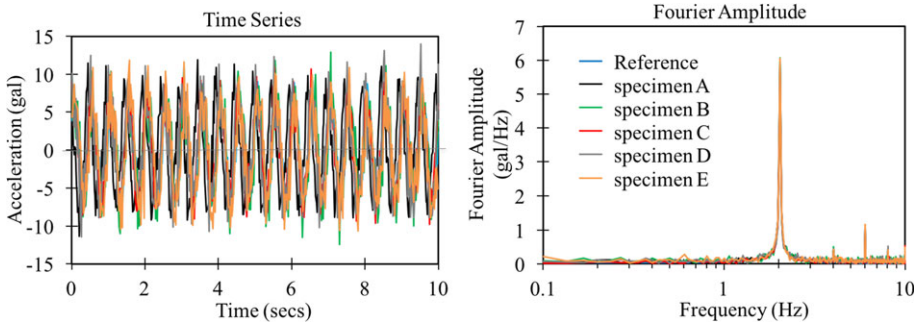

FIGURE 7 Waveform and Fourier-amplitude spectrum after correction (with the frequency of the shaking table set to 2 Hz and the amplitude set to around 10 gal)

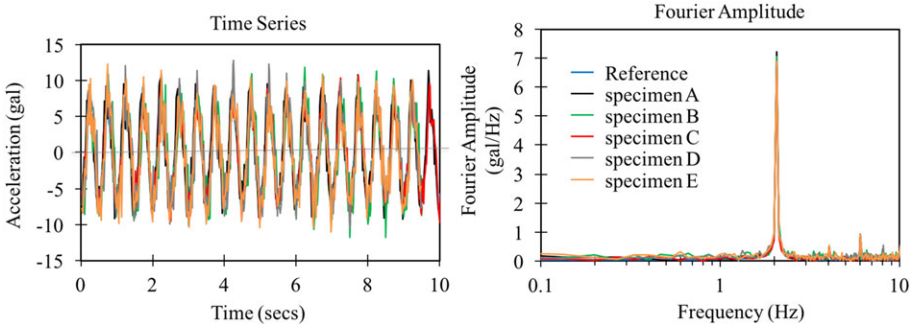

FIGURE 8 Comparison of resampled waveforms and Fourier-amplitude spectra with reference measurements (with the frequency of the shaking table set to 2 Hz and the amplitude set at around 10 gal)

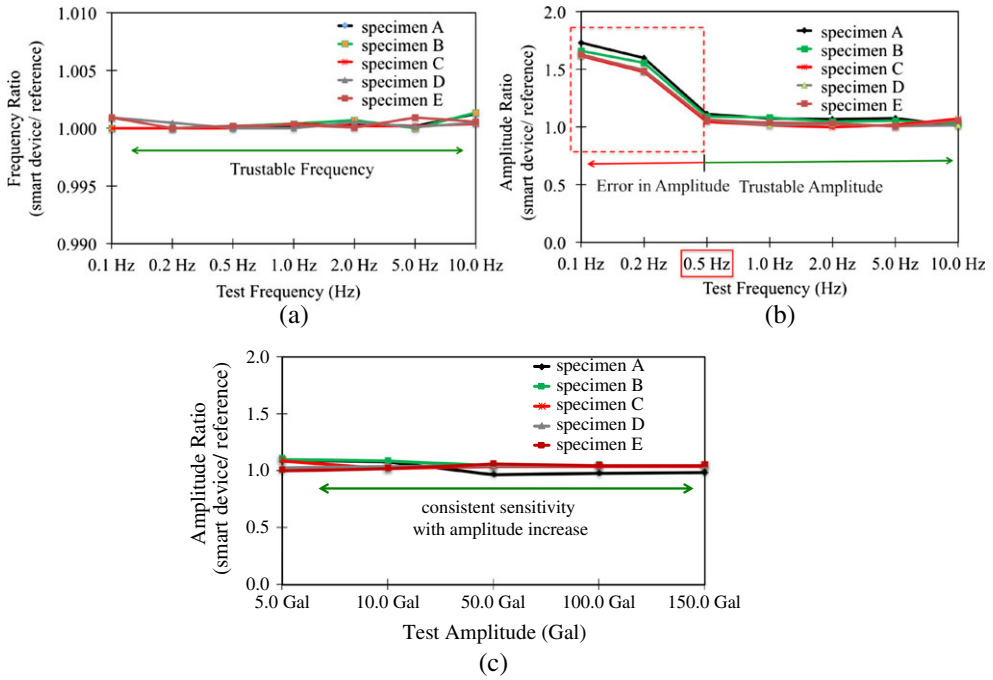

FIGURE 9 (a) Error in frequency measurement, (b) smart-device-to-reference amplitude ratio, and (c) smart-device-to-reference amplitude ratio with amplitude increase

3.5 | Earthquake-wave-excitation tests

In addition to the sinusoidal loading tests, earthquake excitation tests were conducted to evaluate the performance of smart devices in measuring the strong ground motion and the responses of structures. The uniaxial shaking table (SSV-125) was used for input of earthquake waves during the experiment. Each device was fixed on the shaking table along with the high-precision servo-velocity sensor using double-sided adhesive tape as shown in Figure 10.

The shaking table was excited by two different earthquake ground motions—one was measured from the 1995 Kobe Earthquake by the Japan Meteorological Agency Station (KJMA-NS), the other was measured from the 2011 Tohoku Earthquake by the Miyagi-Shiogama Station (MYG012-NS)—with varying characteristics. Experiments were conducted for varying intensity levels of earthquake ground motion (10, 50, 100, 200, 300, and 450 gal for the Kobe wave and 50, 100, 250, and 450 gal for the Miyagi wave), considering the displacement limitation of the shaking table (allowable stroke of $\pm$75 mm).

The earthquake motions recorded by five different smart devices were compared with that recorded by the reference sensor in terms of the acceleration time history, Fourier amplitude, dominant frequency, and 5%-damped-acceleration-response spectra. As with the sinusoidal tests, the acceleration-time-history and frequency-response plots were corrected using the actual average sampling rate of each device.

FIGURE 10 Shaking-table test set-up for earthquake loading

Throughout the whole test, a sampling rate of 100 Hz was adopted for the smart devices and the reference sensor. Figure 11 shows acceleration time history, frequency-domain plot, and 5%-damped-acceleration-response spectra measured by three smart devices and reference sensors for the Miyagi earthquake scaled to 200 gal. It can be seen that smart-device measurements agreed with the reference sensor. The Fourier-amplitude and response-acceleration spectra in each periodic component show almost no difference between the reference sensor and the smart devices. It can be observed that smart devices with respect to the reference sensor are capable of accurately measuring both the predominant frequency and the amplitude of the ground motion.

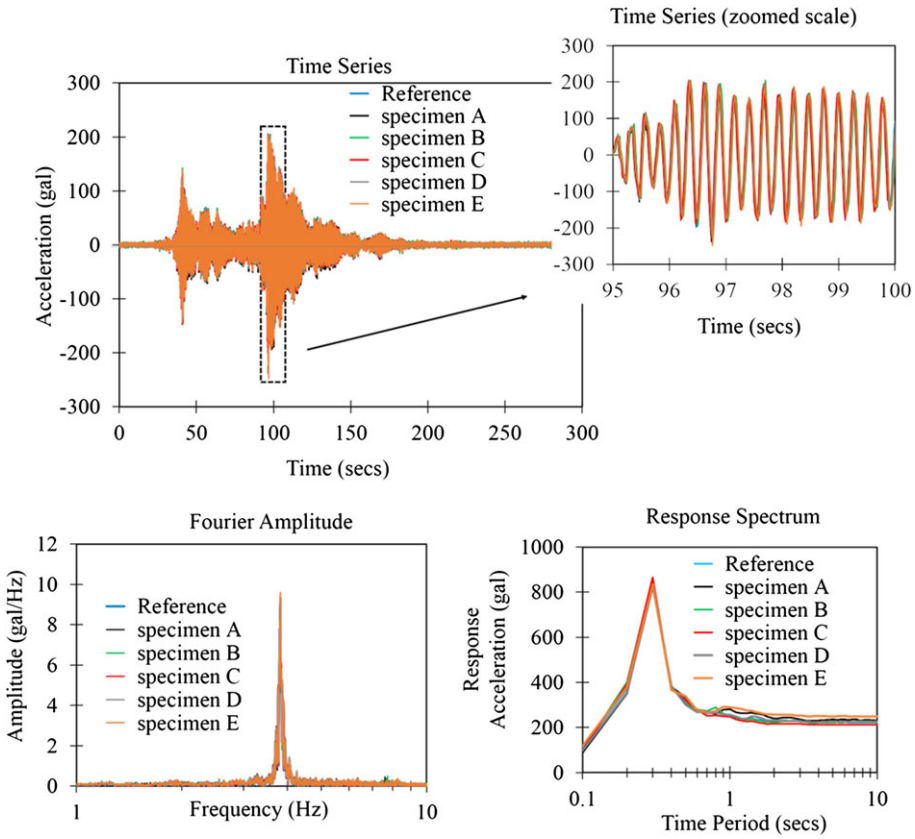

FIGURE 11 Ground motion input-vibration results (5% Miyagi)

3.6 | Trigger function tests

The most basic method for seismic-event observation is to continuously measure and transmit the acceleration data to the server in real time, as with the multiple-record mode shown in Figure 2b. However, this method increases the communication cost, and data management is a major drawback. Therefore, long-term observations using a trigger, as in the trigger recording mode shown in Figure 2c, rather than continuous measurement, seems valid because acceleration data will be recorded and transmitted only during earthquakes. The stability of smart devices for long-term observation is an issue of concern for bridge engineers. Applying unstable systems to real structures such as bridges will increase running costs and compromise practical utility, as accessing a bridge and maintaining the SHM system is not easy.

To implement the above-described trigger function in practice and verify whether it can operate as expected, the structural model test shown in Figure 12a was conducted. Smart devices (iPhone 5s) were fixed at the base and at each story level of the structural model subjected to seismic excitation using double-sided adhesive tape. The acceleration waveform and response of the structural model at different levels measured by different smart devices are shown in Figure 12b.

For small-intensity ground-motion input, only the devices at the upper-story levels (second, third, and fourth) were triggered and started recording, whereas devices at the bottom levels (base and first) were not triggered due to the shaking amplitude is smaller than the threshold. Therefore, it can be known that the trigger function for an individual device is feasible.

However, for a structural monitoring system, the devices connected to a measurement network should be triggered simultaneously, when any of the device/devices is/are triggered. Therefore, in addition to the threshold peak ground acceleration value, the remote trigger (online trigger) to start recording on all devices connected to the same network was implemented using Dropbox Sync API remote communication between devices. It is possible for all smart devices included to a network to communicate with each other without compromising the system resources. As illustrated in Figure 13, when one device is triggered, all other devices will receive the command to be triggered as well, though with little time delay (depends on strength of internet connection). However, this time delay will be covered by the buffering time, and thus, no data loss of the triggered records will occur. Thus, the remote trigger functionality ensures that these individual devices can work together as one system.

4 | APPLICATION CASES TO STRUCTURAL-VIBRATION MEASUREMENT

The smart-device-based system developed in this study has been applied to vibration measurement of real structures with the purpose of evaluating its capability and reliability.

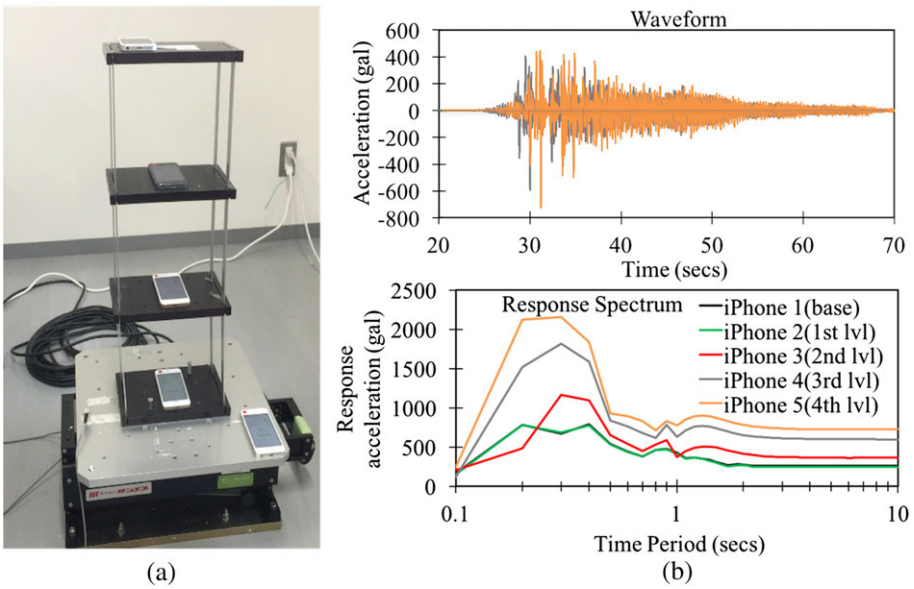

FIGURE 12 (a) Structural-model test and (b) structural-model input-vibration results (Kobe)

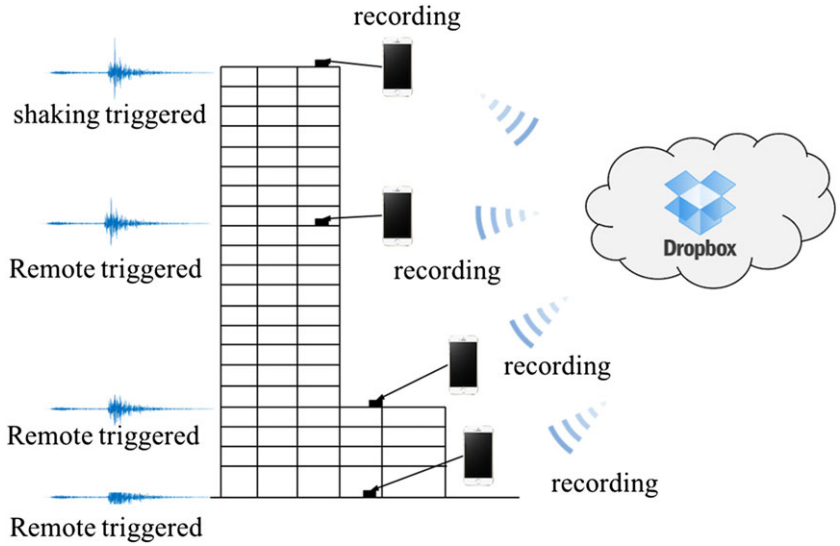

FIGURE 13 Remote triggering method of smart devices to start recording

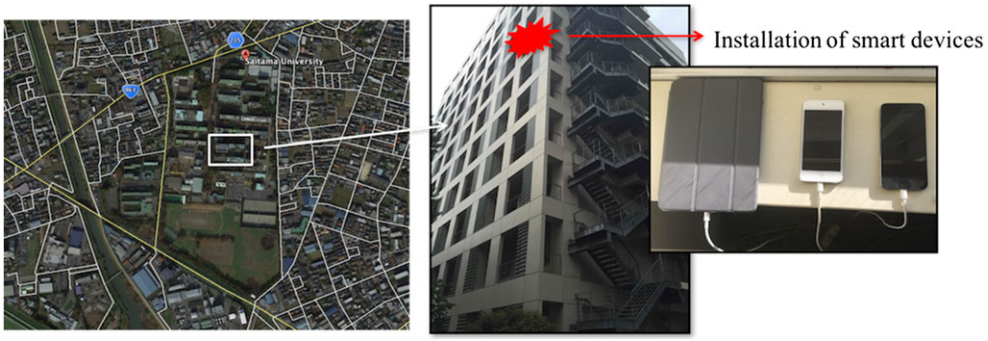

FIGURE 14 Installation of smart devices at eighth floor of a research building at Saitama University

4.1 | An application case to earthquake-response observation at a building

Smart devices were placed at the eighth floor of an 11-story reinforced-concrete-frame building at Saitama University for long-term strong-motion observations from February 2015, as shown in Figure 14. Strong adhesion of smart devices with the structure was ensured using double-sided adhesive tape as used in previous experiments. As for now, the smart devices were triggered by 13 different significant earthquakes. In this paper, four events with relatively larger intensities are chosen to represent the feasibility of earthquake response observation by smart-device based system. The epicenters and the distributions of seismic intensity of the four earthquakes are shown in Figure 15. The acceleration waveforms and Fourier amplitude spectrum along device *X*-axis are shown in Figure 16.

It can be seen that, for all earthquake events, the dominant frequency of the structure at the location of smart-device installation is identified as around 1.2–1.4 Hz, which seems justifiable. This shows that smart devices with the proposed system are also efficient for observing real earthquake events.

However, this application is limited to moderate-to-strong earthquakes. Low-grade consumer devices like smart devices often employ cheap MEMS that does not support low noise to signal ratio due to which continuous noise components of approximately ±5 gal is obtained (as can be seen from Figure 16). It is therefore, difficult to set a low trigger value to allow smaller-magnitude earthquakes to be recorded even though continuous measurements are taken, and accurate waveform data concerning earthquakes with smaller magnitudes are hidden by noise components. Some suggestions in order to improve the proposed system following points could be considered.

1. Each year, smart device makers are always making some kind of improvements in their hardware for better performance and to cope up with the challenging market. Therefore, improvements in the resolution and sensitivity of

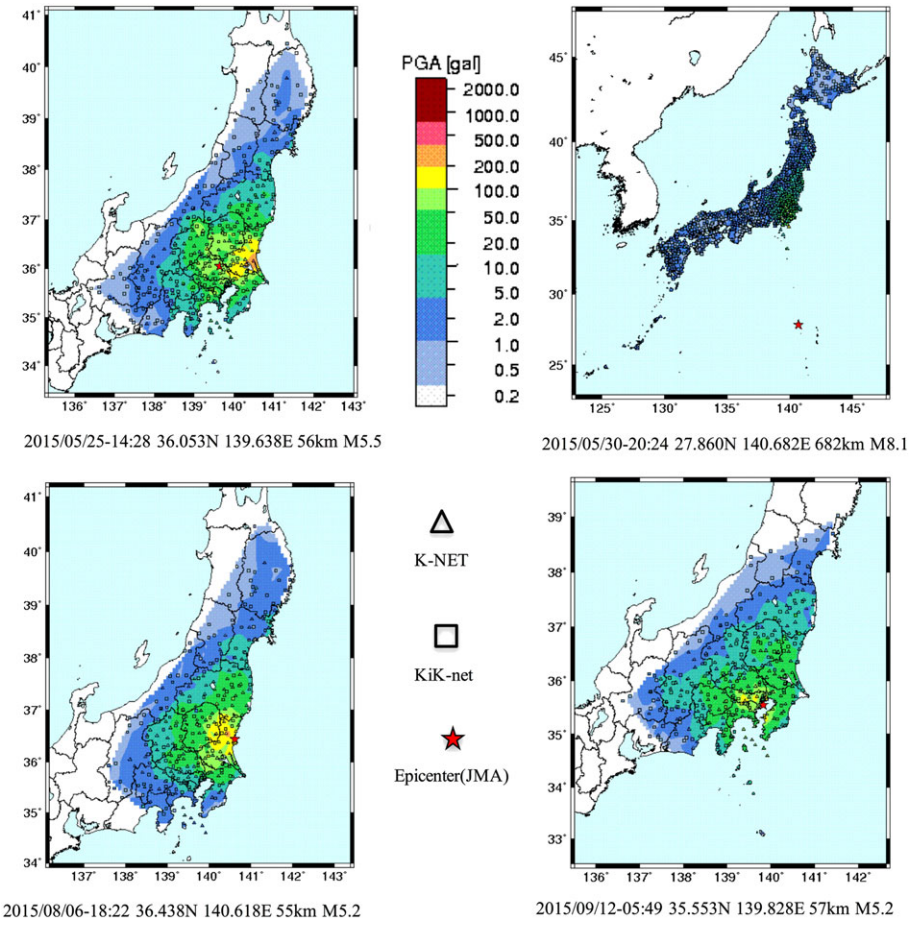

FIGURE 15 Epicenter of the earthquake trigger events (K-NET and KiK-net NIED)

MEMS accelerometers can be expected in the future, which helps the proposed system to be applied for observation of smaller earthquakes.

Meanwhile, the raw data can be processed to reduce the noise components and obtain improved waveform with dominant earthquake components by applying some signal processing techniques. For example, one of the method would be to apply a band-pass Filter to the raw data, where frequency components outside of the scope of the measurement could be eliminated in order to obtain a refined signal with less noise.

4.2 | An application case to environment-vibration measurement of a bridge

The purpose of this test is to evaluate the integrated smart-device-based measurement system in comparison to commercial cable-based structural-monitoring systems in a real bridge instead of a laboratory environment. For this purpose, the Sakitama-Ohasi Bridge located at Toda, Uchiya, Saitama Prefecture, Japan, was considered because cable-stayed bridges are more flexible and therefore can be assumed to be suitable for vibration-based SHM methods to assess their condition. The structure has two spans, 190 m each, and is suspended by cables. It serves as a part of the national highway crossing the Arakawa River.

The bridge was instrumented with six vertical high-quality servo-velocity sensors (VSE-15D, used as a reference) at equal space spanning the longitudinal direction of its first deck. These six sensors were marked from Channel 1 to Channel 6 with closed rectangles as illustrated in Figure 17. An external-battery-power data logger was used to collect vibration data from these six sensors through cables at a sampling rate of 100 Hz. The measurement was conducted during the daytime, due to which most of the vibration record was generated by dynamic traffic loading.

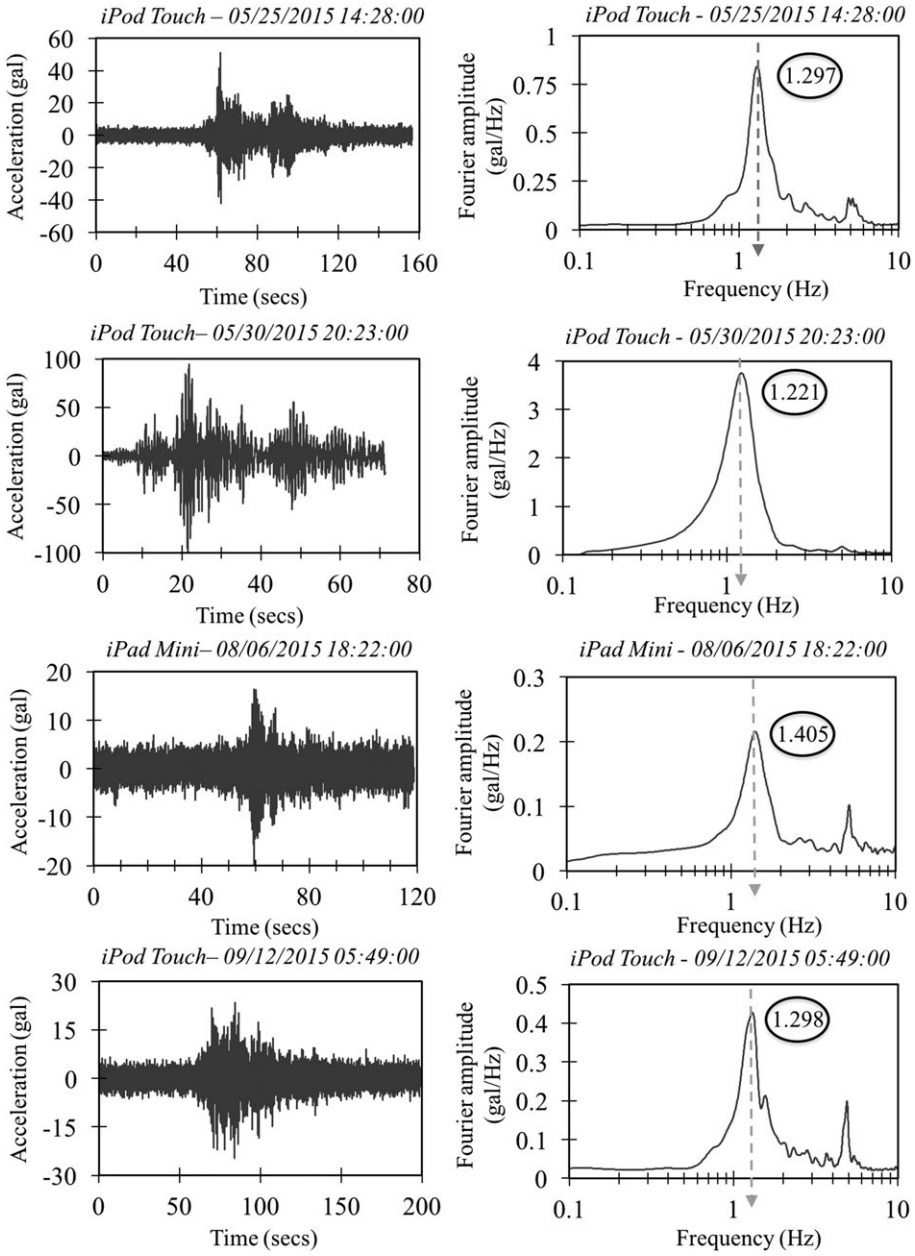

FIGURE 16 Waveform and Fourier-spectrum measurements obtained by smart devices for real earthquakes

These six high-quality sensors are used as references to the smart devices, which were placed adjacent to them. The photos of the data logger and pairs of servo-sensor and smart devices are shown in Figure 18. The smart devices were

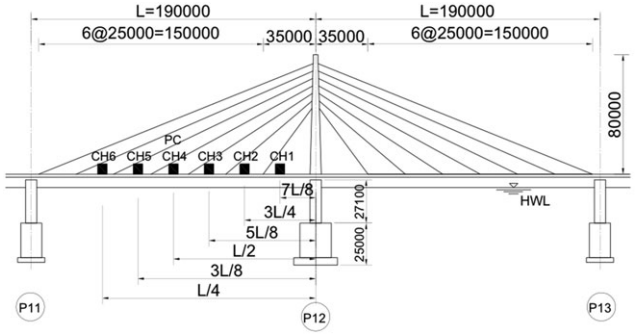

Location	Channel Number	Smart Device Type
7L/8	1	iPod Touch (1)
3L/4	2	iPhone 5s (1)
5L/8	3	iPhone 6 (1)
L/2	4	iPhone 6 (2)
3L/8	5	iPhone 5s (2)
L/4	6	iPod Touch (2)

FIGURE 17 Location of reference-sensor installation and smart devices

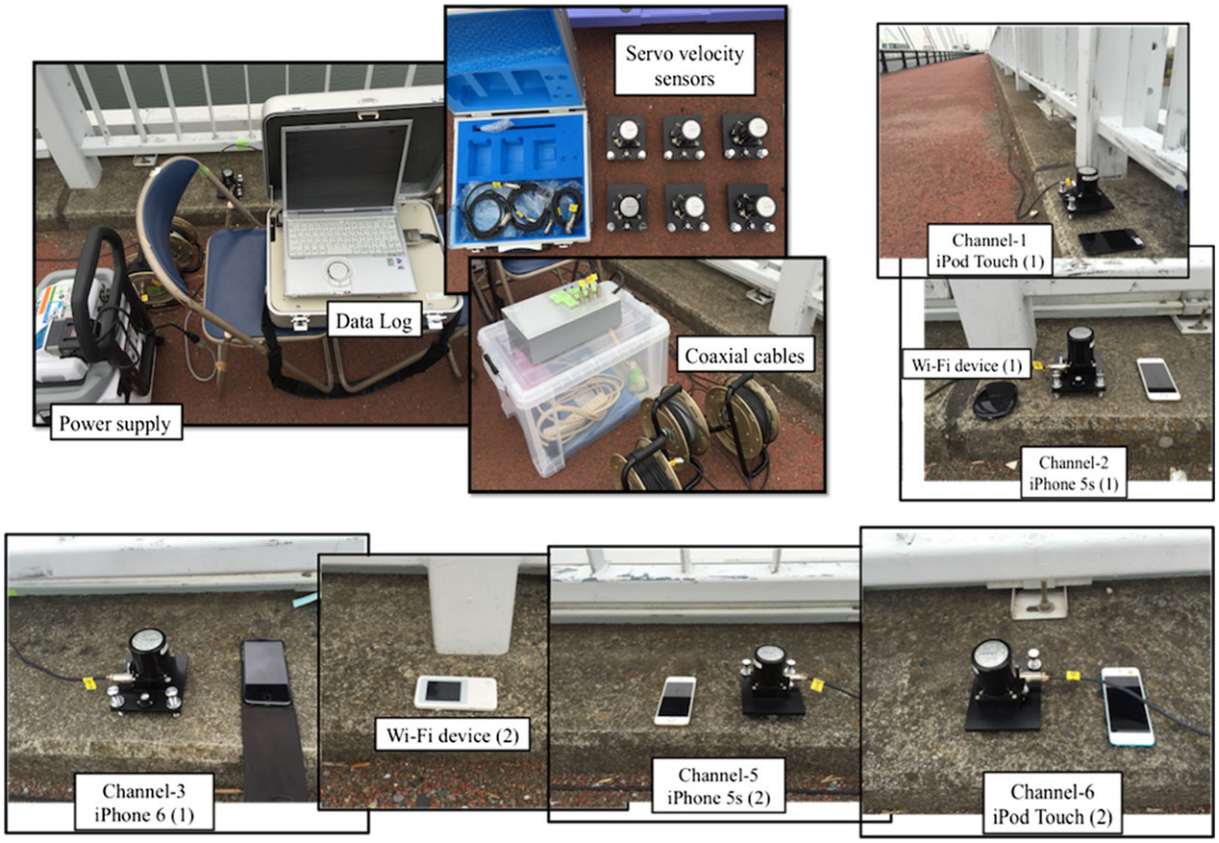

FIGURE 18 Instrumentation involved in the bridge-vibration measurement

fixed via double-sided adhesive tape, ensuring strong bond and no relative movement at the contact surface. Measurement was initiated (started and stopped) manually in the smart devices (iPhone 6 2) installed at the L/2 location, whereas measurement in all other smart devices was initiated automatically using the remote trigger function. Two portable Wi-Fi devices were used to establish a common network between the smart devices.

Acceleration records of the servo-velocity sensors were taken for the purpose of comparing the waveforms and Fourier spectrum of the simultaneous records by the reference sensors and smart devices with the same scale. Because the reference sensors system and the smart devices system were manually controlled, that is, not automatically triggered by designated GPS time, time lag between the records of these two systems exists. The time lag was firstly extracted from the shift time of the peak of cross-correlation waves. Then the whole waveform was moved forward or back with the time length of the extracted time lag. The comparison between the acceleration waveforms recorded by the reference system and the smart device system are shown in Figure 19.

It can be seen that the vertical vibration level of this bridge structure is large, and waveforms of these two system are almost the same. The fast Fourier transform is commonly used to identify dynamic properties of structures in the frequency domain. The fundamental natural frequency can be identified from Fourier spectrum by peak picking method, that is, selecting the frequency corresponding to the first peak. Fourier spectrum of the acceleration records are shown in the right figures in Figure 19. It can be seen clearly from both of the two measurement systems that the fundamental natural frequency of the first span is 0.38 Hz. To validate this result although finite element analysis has not been performed as a part of this study, however, this value of natural frequency is seen to be comparable with the analytical approach developed by Kawashima et al..[34] In that study, relation between lowest natural frequency and span length for cable-stayed bridges is developed through regression analysis which is given by Equation 3.

$$f_1^{\mathrm{BV}} = 33.8\mathrm{L}^{-0.763} \tag{3}$$

where f_1^{BV} is lowest natural frequency for vertical flexural oscillation (Hz) and L is central span length (m; corresponds to 380 m for this bridge).

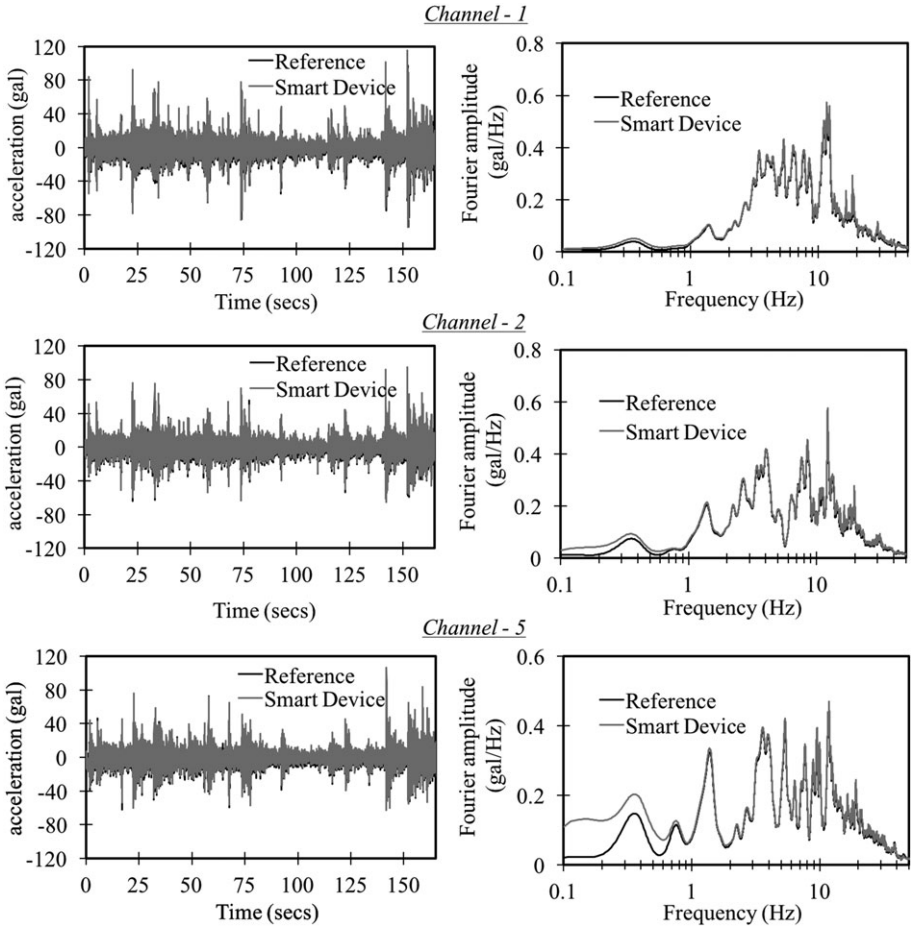

FIGURE 19 Time-history-acceleration records and corresponding Fourier spectra at Channels 1, 2, and 5, as measured by smart devices and reference sensors

The natural frequency computed using Equation 3 is equal to 0.36 Hz that is very close to the experimental natural frequency of 0.38 Hz. For further analytical purposes in the future, the system based on smart devices shall also be tested to see if it can produce valuable modal-identification results for SHM.

5 | CONCLUSIONS

In this paper, an advanced smart-device-based seismic-sensing and structural-response-measuring system was established, and the effectiveness of which has been approved through shaking table test and practical use to seismic response and environment vibration measurements at structures. The validity and accuracy of built-in MEMS accelerometer sensors on the smart devices was confirmed by a series of shaking-table tests involving sinusoidal excitations and scaled ground-motion excitations, what have been known for individual measurement device are concluded as follows.

1. Pink-noise effect of the accelerometer is observed in smart devices resulting in overestimation of the amplitude at low frequency by $1/f$ in the frequency range 0.5–10 Hz. But the difference from the high-precision measuring device was small, and the predominant frequency could be identified clearly. That is to say, the pink-noise will not affect the practical use very much, which has been proved through earthquake-input shaking-table tests that smart devices can monitor earthquake-like random vibrations very well.
2. The observable acceleration level of smart devices is more than 5 gal in the frequency range of 0.1 to 10 Hz
3. The possible sampling rate is 100 Hz. Although the sampling rate is unstable, we can correct the data step using the GPS time.
4. The trigger function to a designed acceleration level is workable.

After the effectiveness and accuracy of individual device have been examined, the measurement system including group devices connected to the same "control center" (Dropbox) is established; based on which the trigger of group sensors, real-time data transport and data acquisition to the a cloud server have been realized. The effectiveness of the measurement system has been approved using structural-model testing and practical use of the developed measurement system to observe seismic response at a building and environment vibration on a bridge structure. The effectiveness of the smart-device-based vibration measurement system are listed as follows.

1. The trigger command can be send to other devices simultaneously as any device/devices is/are triggered. This is the basic of the measurement system that makes the sensors can act as a group through a wireless network and wiring process is unnecessary.
2. The data transport is stable—no data loss happened during the continuous measurement.
3. Dynamic properties extracted from smart-device-based measurement system are compared with those from high-quality sensor system. The possibility of the smart-device-based measurement system has been shown.

In general, the smart-device-based measurement system naturally possess the three prerequisites of a vibration measurement system, that is, sensors, data transfer, and GPS information (location and time). By using smart devices for vibration sensing and seismic monitoring, the proposed technique can offer a dense array of strong-ground-motion and structural-response system that will facilitate studies leading to an improved understanding of the dynamic behavior and potential for damage to structures.

ACKNOWLEDGEMENTS

The authors would like to thank and express gratitude to Prof. Masato Motosaka of Tohoku University, International Research Institute of Disaster Science (IRIDeS), for offering the vibration table of the laboratory used to conduct experiments in the present study.

ORCID

Ashish Shrestha http://orcid.org/0000-0002-6530-1643

REFERENCES

[1] Ghasemi, H., Otsuka, H., Cooper, J. D., and Nakajima, H. (**1996**). Aftermath of the Kobe earthquake. 60(2), 17–22.

[2] K. Kawashima, S. Unjoh, *J. Earthquake Eng.* **1997**, *1*(3), 505.

[3] Y. Kitagawa, H. Hiraishi, *J. Jpn. Asso. Earthquake Eng* **2004**, *4*(3), 1–29. (Special Issue) 2004.

[4] Nakashima, M., Kawashima, K., Ukon, H. and Kajiwara, K. (**2008**). Shake table experimental project on the seismic performance of bridges using E-defense. 14WCEE, *Beijing, China*.

[5] Kawashima, K., Ukon, H., Kajiwara, K. (**2008**). E-defense experiment on the seismic performance of a bridge column built in 1970s. *Proceedings of the 14th World Conference on Earthquake engineering, Beijing 2008*.

[6] Nakashima, M. (**2008**). Roles of large structural testing for the advancement of earthquake engineering. 14WCEE, *Beijing, China*.

[7] Horioka, K. (**2013**). Clarification of mechanism of Shinkansen derailment in the 2011 great East Japan earthquake and countermeasures against earthquakes. JR EAST Technical Review-No.27, pp. 13–16

[8] Takahashi, Y. (**2012**) Damage of rubber bearings and dampers of bridges in 2011 great East Japan earthquake. *Proc. Intl. Symposium on Engineering Lessons Learned from the 2011 Great East Japan Earthquake*

[9] Mihailov, V., Celebi M., and Talaganov K. (**2000**). Seismic monitoring of structures – An important element of seismic hazard reduction. *Proc., 12th World Conf. Earthquake Eng*., New Zealand.

[10] Spencer Jr., B. F., Sandoval, M. R., Kurata, N. (**2004**). Smart sensing Technology for Structural Health Monitoring. *13th World Conference on Earthquake Engineering. Vancouver, B.C., Canada, August 1–6, 2004*. Paper No. 1791

[11] J. A. Rice, K. A. Mechitov, S. H. Sim, B. F. Spencer Jr., G. A. Agha, *Struct. Control Health Monit.2011* **2010**, *18*, 574.

[12] R. W. Clayton, T. Heaton, M. Kohler, M. Chandy, R. Guy, J. Bunn, *Seismol. Res. Lett.* **2015**, *86*(5), https://doi.org/10.1785/0220150094.

[13] Nagayama, T., and Spencer Jr., B. F. (**2007**). Structural health monitoring using smart sensors. NSEL Report Series. Report No. NSEL-001

[14] C. R. Farrar, G. Park, D. W. Allen, M. D. Todd, *Struct. Control Health Monit.* **2006**, *13*, 210.

[15] B. F. Spencer Jr., M. E. Ruiz-Sandoval, N. Kurata, *Struct. Control Health Monit.* **2004**, *11*, 349.

[16] Ericsson Mobility Report (**2014**): On the pulse of the networked society

[17] Dashti, S., Reilly, J., Bray, J. D., Bayen, A., Glaser, S., and Mari, E. (**2011**). iShake: Using personal devices to deliver rapid semi-qualitative earthquake shaking information. Technical report G10AP00006, Department of Civil and Environmental Engineering, University of California, Berkeley, CA, USA, February 2011. Available online: <http://earthquake.usgs.gov/research/external/reports/G10AP00006.pdf.%3e

[18] Morgenthal, G. (**2012**). The application of smartphones in bridge inspection and monitoring. 18th Congress of IABSE, Seoul, 2012

[19] G. Morgenthal, H. Hopfner, *J. Civil Struct. Health Monitor.* **2012**, https://doi.org/10.1007/s13349-012-0025-0.

[20] S. Naito, H. Azuma, S. Senna, M. Yoshizawa, H. Nakamura, K. X. Hao, H. Fujiwara, Y. Hirayama, N. Yuki, M. Yoshida, *J. Disaster Res.* **2013**, *8*(5).

[21] J. Reilly, S. Dashti, M. Ervasti, J. D. Bray, S. D. Glaser, A. M. Bayen, *IEEE Trans. Automat. Sci. Eng.* **2013**, *10*(2), 242.

[22] M. Feng, Y. Fukuda, M. Mizuta, E. Ozer, *Sensors* **2015**, *15*, 2980, https://doi.org/10.3390/s150202980.

[23] H. Yoon, H. Elanwar, H. Choi, G. M. Fard, B. F. Spencer Jr., *Struct. Control Health Monit.* **2016**, *23*, 1405.

[24] Apple Inc. iOS developer library (**2012**). "MotionGraphs" Version 1.0.1 <https://developer.apple.com/library/ios/samplecode/MotionGraphs/Introduction/Intro.html%3e

[25] Dropbox, Dropbox Developer, Sync API. (**2014**). <https://www.dropbox.com/developers/sync%3e

[26] APS-113 ELECTRO-SEIS® APS Dynamics, Inc. (**2014**) <http://www.apsdynamics.com/images/stories/Prospekte/APS_Shaker/APS_113__APS_113-HF/APS_113_HF_Data_Sheet_en.pdf%3e

[27] SAN ES Corporation (**2015**) <http://www.san-esu.com/product010_06.html%3e

[28] Bosch Sensortech, Reutlingen, Germany. (**2011**). BMA220 – Digital, triaxial acceleration sensor. rev. 1.10.

[29] Bosch Sensortech, Reutlingen, Germany. (**2014**). BMA280 – Digital, triaxial acceleration sensor. rev. 1.8.

[30] Wikipedia contributors. (**2016**). Comparison of smartphones. *Wikipedia, The Free Encyclopedia*, Available online <http://en.wikipedia.org/wiki/Comparison_of_ smartphones>

[31] Servo velocity sensor specifications. <https://www.to-soku.co.jp/products/servo/index.html%3e

[32] STMicroelectronics, Geneva, Switzerland. (**2009**). LIS331DLH – MEMS digital output motion sensor. doc id 15094 rev 3 edition.

[33] R. Amick, J. Patterson, M. Jorgensen, *International Journal of Applied Science and Technology* **2013**, *3*(2)*, February 2013*.

[34] K. Kawashima, S. Unjoh, H. Mukai, in *Proceedings of the Earthquake Engineering Workshop, Japan Society of Civil Engineers* **1993**, *22*, 511. (in Japanese)

How to cite this article: Shrestha A, Dang J, Wang X. Development of a smart-device-based vibration-measurement system: Effectiveness examination and application cases to existing structure. *Struct Control Health Monit*. 2018;25:e2120. https://doi.org/10.1002/stc.2120